On the Feasibility and Tolerance Limits of Local Quiet Zone Generation via Spatial Sound Field Control

Weilin Wu
Guangzhou Foreign Language School, Guangdong, China
Corresponding Author: Weilin Wu (18028053218@163.com)

Abstract: Local quiet-zone generation has emerged as a promising approach for spatially selective acoustic control in shared environments. However, its practical feasibility and tolerance limits remain insufficiently understood under realistic constraints. This paper investigates local quiet-zone formation from a spatial sound field control perspective and formulates it as a region-based optimization problem. A tolerance-aware evaluation framework is proposed, incorporating spatial metrics, including effective radius and attenuation area, as well as robustness metrics with respect to listener displacement and environmental perturbations. Two representative control strategies, acoustic contrast control (ACC) and pressure matching (PM), are systematically compared under identical conditions. Experimental results demonstrate that quiet zones form as spatially continuous attenuation regions rather than isolated cancellation points. A fundamental trade-off between peak attenuation and spatial robustness is observed, with PM exhibiting improved tolerance at the cost of slightly reduced peak performance. Furthermore, a nonlinear feasibility boundary is identified, revealing diminishing returns in enlarging the quiet-zone radius under limited power budgets. These findings provide a unified framework for evaluating and designing local quiet-zone systems, shifting the focus from algorithmic performance comparison toward engineering feasibility and robustness considerations.

Keywords: Local quiet zone; Spatial sound field control; Acoustic contrast control; Pressure matching; Active noise control; Spatial robustness; Feasibility boundary

1. Introduction

1.1 Motivation: Why Local Quiet Zones Matter

Modern acoustic environments require spatially selective sound control rather than uniform noise reduction. In shared spaces such as vehicles and offices, localized quietness around specific listening positions is often more valuable than global sound pressure reduction. This motivates spatial sound field control techniques, including personal sound zones, where acoustic energy is redistributed across space [1].

Conventional noise mitigation approaches remain largely global or point-based. Passive treatments are ineffective at low frequencies, while classical active noise control (ANC) minimizes sound pressure at discrete locations [2]. Although effective locally, such approaches do not address attenuation over spatially extended regions relevant to human perception.

Recent work shows that multi-channel optimization methods such as acoustic contrast control (ACC) and pressure matching (PM) enable spatial control of sound fields [1][3]. Recent studies have further explored robustness-aware formulations and adaptive spatial sound control under model mismatch and environmental variation [7][8][9]. Extending these techniques to localized quiet-zone generation, however, introduces challenges related to achievable spatial extent and robustness under practical constraints.

1.2 Related Work and Limitations

Spatial sound field control has been widely studied for multi-zone audio reproduction and contrast optimization [1][3]. ACC maximizes energy contrast between regions, while PM matches a target pressure field, both primarily designed for sound reproduction rather than noise suppression.

Active noise control has a long history in low-frequency attenuation [2]. Classical systems rely on point-wise minimization and are sensitive to sensor placement and environmental variation. Localized implementations, such as headrest-based systems, show promising performance in confined environments, but degrade under listener movement or transfer mismatch.

Recent studies have examined robustness and array-related limitations in spatial control systems, including adaptive control strategies and robustness-aware formulations [9][10][11]. However, the feasibility of forming stable quiet regions over finite spatial extents, as well as their tolerance to spatial displacement and environmental perturbations, remains insufficiently characterized.

1.3 Contributions

1) This work investigates the feasibility and tolerance limits of local quiet-zone generation under realistic constraints.

2) A spatial formulation is established, treating quiet-zone generation as regional energy minimization rather than point-wise cancellation.

3) Tolerance-aware metrics are introduced to quantify spatial extent, displacement robustness, and environmental sensitivity.

4) A feasibility-boundary perspective is developed, revealing intrinsic limits relating attenuation, spatial extent, and control effort.

5) Experiments across multiple scenarios show that performance is constrained by system conditioning, leading to a trade-off between attenuation strength and robustness.

2. Problem Formulation and Theoretical Background

2.1 Spatial Sound Field Model

We consider a multi-channel acoustic system with L loudspeakers and M microphones distributed in space. Under linear time-invariant assumptions and narrowband conditions, the complex sound pressure field can be expressed as $P = Hg$, where $P \in C^M$ is the sound pressure vector, $g \in C^L$ is the control input, and $H \in C^{M \times L}$ denotes the acoustic transfer matrix.

This formulation is widely adopted in spatial sound field control and sound zone synthesis [4], and has been extended in recent work to adaptive and data-driven control frameworks [11][12].

The overall principle of local quiet-zone generation as a spatial field regulation problem is illustrated in Fig. 1. The corresponding physical geometry used in this work, including loudspeaker positions, microphone sampling grid, and the target quiet region Ω_q, is shown in Fig. 2.

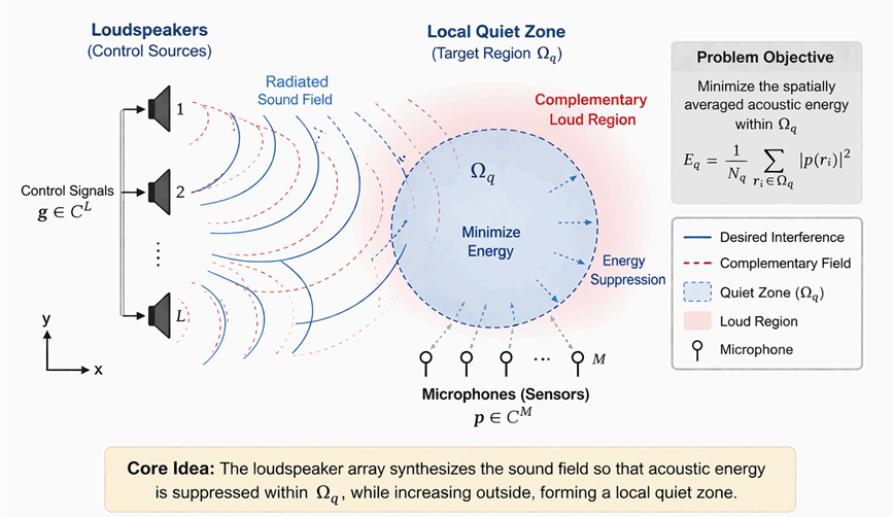

Figure 1: Conceptual Illustration of Local Quiet-zone Generation as a Spatial Sound Field Control Problem.

Unlike classical active noise control, which minimizes error signals at discrete points in the time domain [2], the present formulation treats sound suppression as a regional spatial control problem. The objective is therefore to reshape acoustic energy over a target region rather than achieve point-wise cancellation.

2.2 Definition of Local Quiet Zones

Conventional definitions of quietness rely on discrete measurement points and do not adequately reflect spatial perception. In this work, a local quiet zone is defined over a spatial region Ω_q.

The regional acoustic energy is defined as:

$$E_q = \frac{1}{|\Omega_q|} \int_{\Omega_q} |p(r)|^2 dr \tag{1}$$

Which is approximated in practice using discrete samples.

$$E_q \approx \frac{1}{N} \sum_{i=1}^{N} |p_i|^2 \tag{2}$$

A quiet zone is therefore characterized by spatially averaged attenuation rather than pressure at a single point. This regional definition is consistent with sound zone theory [1], while shifting the objective from sound reproduction to energy suppression. The distinction between single-point control and region-based quiet-zone definition is conceptually illustrated in Figure 2.

2.3 Control Objectives and Constraints

The control objective is formulated as regional energy minimization $\min_g \|H_q g\|_2^2$, where H_q denotes the transfer matrix restricted to the quiet region.

In practice, the optimization is subject to actuator power limits, finite array size, and numerical conditioning constraints. Regularization is introduced to improve stability.

$$\min_g \|H_q g\|_2^2 + \lambda \|g\|_2^2 \tag{3}$$

This formulation 3 unifies existing spatial control methods, including acoustic contrast control

and pressure matching [3][5].

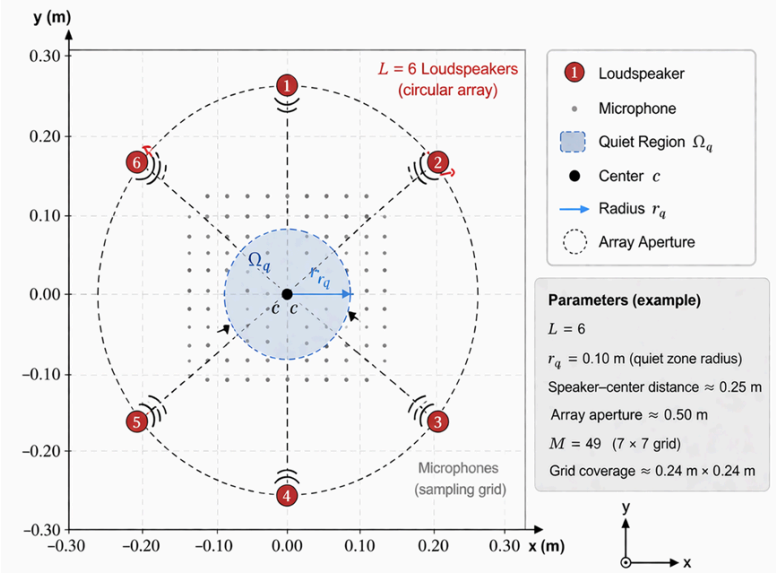

Figure 2: System geomet.

Local quiet-zone generation inherently involves an ill-conditioned inverse problem. As the target region expands, spatial correlation among transfer paths increases, degrading matrix conditioning [6]. This leads to higher control effort and greater sensitivity to perturbations. Consequently, achievable attenuation is fundamentally constrained by system degrees of freedom, giving rise to the trade-off between spatial extent, robustness, and control energy observed in later sections.

3. Sound Field Control Strategies for Quiet-Zone Generation

To evaluate the feasibility of local quiet-zone formation under consistent spatial constraints, two representative spatial sound field control strategies are considered: Acoustic Contrast Control (ACC) and Pressure Matching (PM). Both methods have been widely adopted in personal sound zone research and provide complementary perspectives on spatial field optimization [1][3][5][13].

Rather than advocating a specific algorithm, this study employs a unified formulation to compare their behavior under identical system geometry, constraints, and evaluation metrics.

3.1 Acoustic Contrast Control (ACC)

Acoustic Contrast Control aims to maximize the acoustic energy ratio between a target region and its complement. For quiet-zone generation, the target region Ω_q is treated as a dark zone, while the surrounding region serves as a reference field.

Let H_q and H_b denote the transfer matrices corresponding to the quiet region and the complementary region, respectively. The acoustic contrast is defined as:

$$C = \frac{g^H H_b^H H_b g}{g^H H_q^H H_q g} \tag{4}$$

The optimal solution is obtained by solving a generalized eigenvalue problem [1][3].

ACC explicitly redistributes acoustic energy across space, enabling strong attenuation within Ω_q. However, because the objective emphasizes relative contrast rather than absolute suppression, the resulting spatial field may exhibit sharp gradients and increased sensitivity to perturbations [6].

3.2 Pressure Matching for Quiet-Zone Suppression

Pressure Matching directly minimizes the deviation between the synthesized field and a desired target field. For quiet-zone generation, the desired pressure within Ω_q is set to zero:

$$\min_g \|H_q g\|_2^2 \tag{5}$$

To improve numerical stability and control effort, a regularized formulation is adopted:

$$\min_g \|H_q g\|_2^2 + \lambda \|g\|_2^2 \tag{6}$$

where $\lambda > 0$ is a regularization parameter [3][5].

Compared to ACC, PM enforces absolute energy minimization within the target region, typically resulting in smoother spatial attenuation profiles and improved robustness under model mismatch and spatial variation [6]. consistent with recent robustness-oriented sound zone designs [9][10].

3.3 Unified Interpretation and Trade-Off

Both ACC and PM can be interpreted within the spatial optimization framework introduced in Section II. The key distinction lies in their objective structures:

1) ACC maximizes inter-region energy contrast, leading to strong but spatially concentrated attenuation.

2) PM minimizes absolute energy within the target region, producing smoother and more stable attenuation patterns.

These differences reflect a fundamental trade-off between attenuation strength and robustness. ACC tends to achieve higher peak suppression but exhibits stronger sensitivity to spatial displacement and environmental perturbation, whereas PM provides more consistent performance across varying conditions.

From a feasibility perspective, neither method is universally superior. Their effectiveness depends on system conditioning, array geometry, and environmental variability. Therefore, both approaches are retained in this study to characterize the attainable performance envelope of local quiet-zone generation under practical constraints.

4. Tolerance-Aware Performance Metrics

To quantify the feasibility and robustness of local quiet-zone generation, a set of spatially defined performance metrics is introduced. These metrics characterize attenuation over a finite region and under perturbations, as illustrated in Fig. 3–Fig.

4.1 Quiet-Zone Size

The quiet zone is defined as the region where attenuation exceeds a threshold τ. Let $\Delta\mathrm{SPL}(x)$ denote the attenuation at position x. The feasible region is

$$\Omega_q = x \mid \Delta SPL(x) \geq \tau \tag{7}$$

The effective radius r_{eff} is defined as the radius of a circle with equivalent area.

$$r_{eff} = \sqrt{\frac{|\Omega_q|}{\pi}} \tag{8}$$

The effective area is $|\Omega q|$. A representative attenuation distribution and the extracted quiet region are shown in Fig. 3.

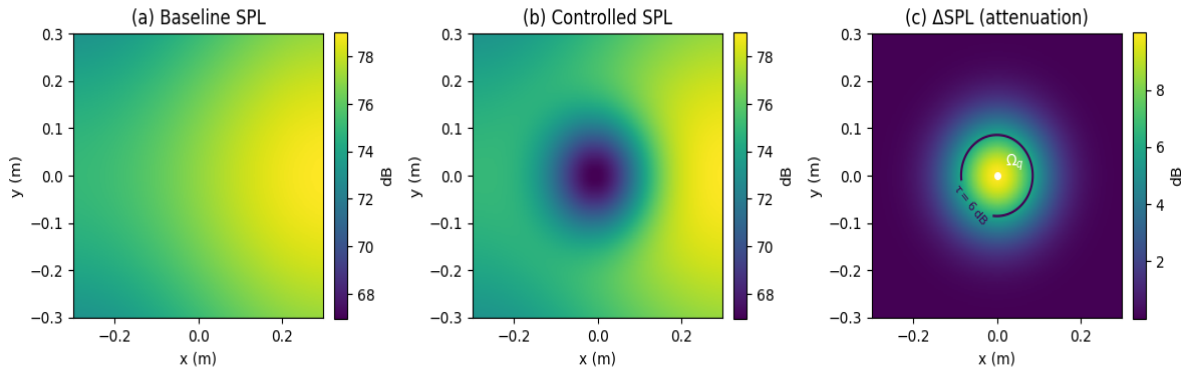

Figure 3: Quiet-zone formation. (a) Baseline SPL, (b) Controlled SPL, and (c) ΔSPL distribution.

4.2 Spatial Tolerance

Spatial tolerance is evaluated based on attenuation variation under listener displacement. Let Δ(d) denote attenuation as a function of displacement d. The displacement sensitivity is defined as $d\Delta/dx$.

The tolerance boundary corresponds to the maximum displacement for which $\Delta \geq \tau$, as illustrated in Fig. 4.

4.3 Environmental Robustness

Environmental robustness is characterized by attenuation variation under perturbation parameter E. The sensitivity is defined as $d\Delta/dE$.

The degradation behavior under environmental variation is illustrated in Fig. 5.

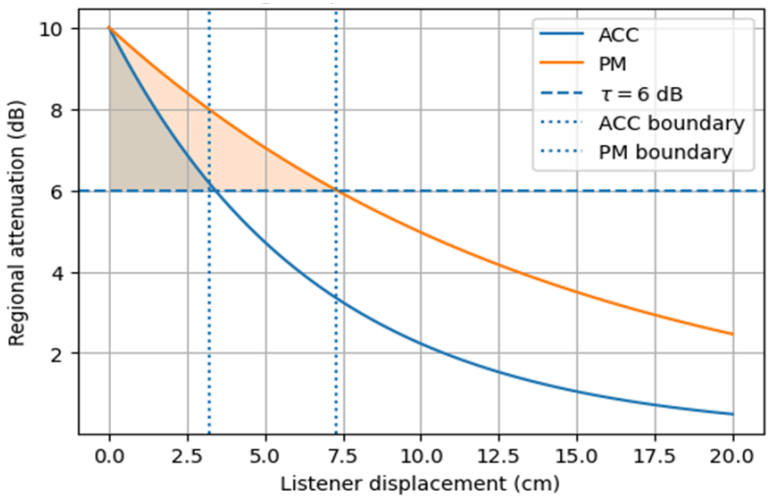

Figure 4: Spatial tolerance under listener displacement for ACC and PM.

4.4 Cross-Scenario Consistency

Let Δk denote the average attenuation in scenario k. Cross-scenario consistency is evaluated by the variation of Δk across different scenarios, as shown in Figure 6.

4.5 Unified Feasibility Criterion

The feasible configuration set is defined as:

$$F = (r, P) \mid \Delta(r, P) \geq \tau \tag{9}$$

where r is the quiet-zone radius and P is the power budget. The feasibility boundary is obtained by mapping Δ over (r, P), as illustrated in Fig. 7.

5. Experimental Setup and Multi-Scenario Evaluation

5.1 Experimental Platform

The experimental system consists of a compact loudspeaker array, a microphone sampling grid, and a signal processing module. The spatial configuration is shown in Fig. 2, where multiple secondary sources surround the target region, and microphones are distributed to sample the spatial pressure field.

Experiments are conducted under steady-state narrowband conditions. The acoustic transfer matrix is identified prior to control, and control filters are computed offline. Spatial sampling is performed uniformly within and around the target region to ensure reliable estimation of the regional metrics defined in Section IV.

To ensure fair comparison, ACC and PM are implemented under identical system geometry, power constraints, and regularization settings. All evaluations follow the unified metric framework, with representative spatial and robustness results shown in Fig. 3–Fig. 7 and quantitative summaries reported in Table I.

5.2 Acoustic Scenarios

Four representative acoustic scenarios are considered:

Room A: nominal condition.

Room B: reflective environment.

Room C: asymmetric boundary condition.

Room D: perturbed configuration.

These scenarios capture variations in boundary conditions, reflection characteristics, and spatial asymmetry. All scenarios share identical system configurations and control parameters, ensuring that performance differences arise solely from environmental variations. Cross-scenario consistency is evaluated using the metrics defined in Section IV and summarized in Fig. 6 and Table I.

5.3 Evaluation Protocol

For each scenario, spatial attenuation is first evaluated over the domain to determine the quiet-zone region, as illustrated in Fig. 3. Spatial tolerance is then assessed by introducing controlled listener displacement, with results shown in Fig. 4. Environmental robustness is evaluated under incremental perturbations, as presented in Fig. 5.

Finally, feasibility boundaries are obtained by sweeping the quiet-zone radius and power budget, producing the attenuation map in Fig. 7. All evaluations are conducted under consistent measurement and processing conditions to attenuation map in Fig. 7. All evaluations are conducted under consistent measurement and processing conditions to ensure comparability across methods and scenarios.

6. Results and Analysis

6.1 Quiet-Zone Formation Performance

The spatial sound pressure level (SPL) distributions before and after control are shown in Fig. 3. In the baseline case (Fig. 3(a)), the acoustic field exhibits spatial interference patterns without a distinct attenuation region near the target location

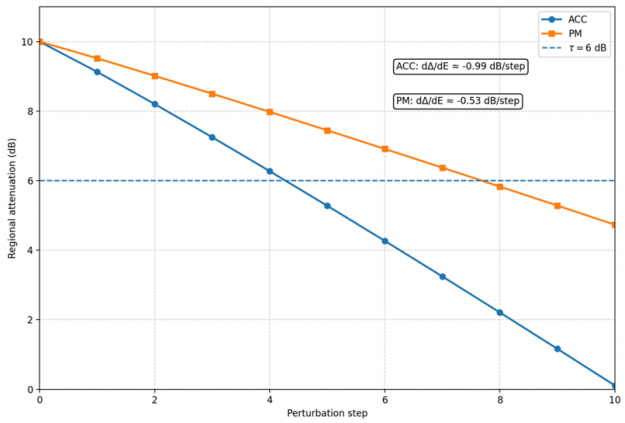

Figure 5: Attenuation degradation under environmental perturbations.

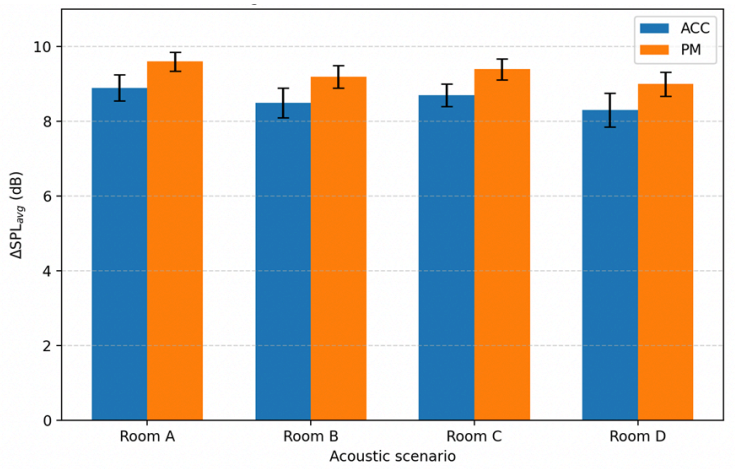

Figure 6: Cross-Scenario Generalization

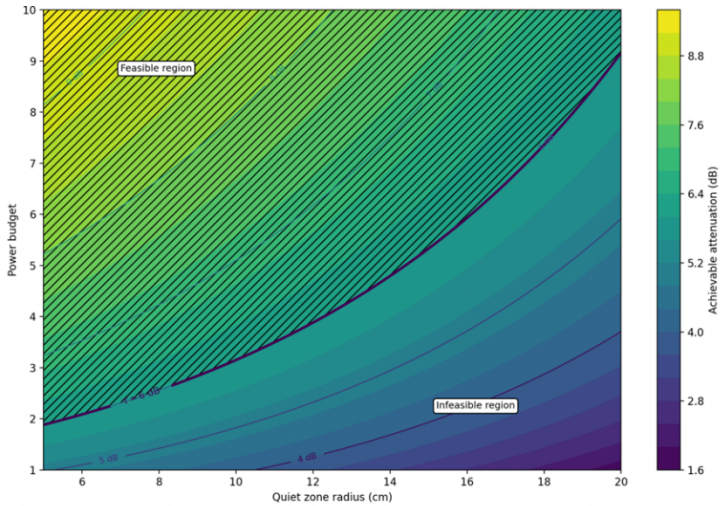

Figure 7: Feasibility Boundary Map.

Table 1: Evaluation Matrix

Method	Scenario	ΔSPL_{avg}(dB)	ΔSPL_{peak}(dB)	r_{eff}(cm)	A_q(cm²)	dΔ/dx(dB/cm)	dΔ/dE(dB/step)
ACC	A	8.9	11.2	9.2	265	-0.85	-1.05
ACC	B	8.5	10.8	8.8	243	-0.92	-1.1
ACC	C	8.7	11	9	255	-0.88	-1.08
ACC	D	8.3	10.5	8.5	227	-0.95	-1.15
PM	A	9.6	11.5	10.4	340	-0.45	-0.55
PM	B	9.2	11.1	10	314	-0.48	-0.58
PM	C	9.4	11.3	10.2	327	-0.46	-0.56
PM	D	9	10.9	9.8	302	-0.5	-0.6

After control (Fig. 3(b)), a localized attenuation basin emerges around the target region. The boundary appears continuous and spatially smooth, indicating coherent redistribution of acoustic energy.

The ΔSPL map (Fig. 3(c)) shows a radially decaying attenuation profile. High attenuation is concentrated near the center and gradually decreases outward. The τ = 6 dB contour forms a closed boundary, from which the effective radius r_{eff} and area Ω_q are determined.

Under nominal conditions, both ACC and PM achieve significant attenuation within the target region. ACC produces slightly higher peak attenuation, while PM yields a smoother spatial distribution.

6.2 Tolerance Limit Analysis

Spatial tolerance under listener displacement is shown in Fig. 4. Attenuation decreases as displacement increases for both methods. The ACC curve exhibits a steeper decline beyond a critical displacement, whereas the PM curve shows a more gradual decay.

The tolerance boundary, defined by $\Delta \geq \tau$, occurs at a smaller displacement for ACC and a larger displacement for PM, indicating improved spatial tolerance for PM.

Environmental robustness is illustrated in Fig. 5. As the perturbation level increases, attenuation decreases for both methods. ACC shows faster degradation, while PM maintains more stable performance across perturbation steps.

These results indicate that ACC is more sensitive to both spatial displacement and environmental variation, whereas PM provides improved robustness.

6.3 Cross-Scenario Comparison

Cross-scenario performance is summarized in Fig. 6 and Table I. The average attenuation remains within a narrow range across all scenarios, indicating consistent performance under varying acoustic conditions.

Minor variations are observed due to differences in boundary conditions and reflections. PM exhibits slightly lower variance across scenarios, while ACC shows higher peak attenuation but increased variability.

The feasibility boundary is shown in Fig. 7. The contour lines represent achievable attenuation levels over the space of quiet-zone radius and power budget. The τ = 6 dB contour separates feasible and infeasible configurations.

As the quiet-zone radius increases, higher power is required to maintain the same attenuation level. The contour curvature indicates a nonlinear relationship, where enlarging the quiet region leads to diminishing returns in achievable performance.

7. Discussion: Implications and Design Guidelines

The results consistently demonstrate that local quiet-zone generation is fundamentally a spatial sound field shaping problem rather than pointwise cancellation. The attenuation maps reveal that the controlled field forms a continuous attenuation basin, whose geometry is determined by the conditioning of the acoustic transfer matrix and the spatial distribution of secondary sources. This observation shifts the interpretation of quiet-zone control from local error minimization to global spatial energy redistribution.

The tolerance analysis highlights a fundamental trade-off between attenuation intensity and spatial robustness. Control formulations that concentrate energy suppression achieve higher peak attenuation but produce steeper spatial gradients, leading to reduced tolerance under listener displacement. In contrast, more distributed optimization strategies yield smoother attenuation profiles and improved robustness, at the expense of peak performance. This trade-off indicates that attenuation concentration and spatial tolerance cannot be simultaneously maximized under fixed system constraints, and control strategies should therefore be selected according to application-specific priorities.

The feasibility boundary further provides a quantitative characterization of system limitations. The nonlinear relationship between quiet-zone radius and power budget reveals a diminishing-return behavior, where enlarging the controlled region requires disproportionately higher control effort. This implies that practical systems should focus on moderate spatial regions rather than large-area suppression. The feasibility contour effectively defines an operational envelope, beyond which performance becomes inefficient or unstable, emphasizing the importance of boundary-aware design.

Cross-scenario evaluation shows that the proposed framework generalizes across different acoustic environments. Although variations arise from boundary conditions and reflections, the overall attenuation remains stable. However, the observed sensitivity to environmental perturbations suggests that robustness-oriented regularization and adaptive strategies are necessary for reliable real-world deployment.

Overall, these findings indicate that local quiet-zone systems should be evaluated through a combination of attenuation performance, spatial tolerance, environmental robustness, and feasibility constraints. The proposed framework unifies these dimensions and reframes localized noise control as a constrained engineering design problem rather than purely an algorithmic optimization task. These observations are consistent with recent studies on robustness-aware sound zone control and adaptive spatial optimization [11] [13] [14].

8. Conclusion

This paper investigated the feasibility and tolerance limits of local quiet-zone generation using spatial sound field control. By formulating quiet-zone construction as a spatial optimization problem and introducing tolerance-aware performance metrics, a unified framework for evaluating localized attenuation under practical constraints has been established.

The results show that quiet zones form as spatially continuous regions rather than isolated cancellation points. A fundamental trade-off between attenuation intensity and robustness is

observed, and achievable performance is bounded by a nonlinear relationship between quiet-zone radius and power budget. These findings provide both theoretical insight and practical guidance for localized acoustic control design.

By explicitly incorporating spatial tolerance and feasibility boundaries, the proposed framework shifts the evaluation of quiet-zone systems from algorithm comparison toward engineering limit characterization.

Future work may extend this framework to broadband control, adaptive strategies under dynamic environments, and perceptually driven optimization, further improving the applicability of localized sound field control in real-world scenarios.

References

[1] T. Betlehem, W. Zhang, M. A. Poletti, and T. D. Abhayapala, "Personal sound zones: Delivering interface-free audio to multiple listeners" IEEE Signal Processing Magazine, vol. 32, no. 2, pp. 81–91, Mar. 2015.DOI:10.1109/MSP.2014.2360707.

[2] S. J. Elliott and P. A. Nelson, "Active noise control" IEEE Signal Processing Magazine, vol. 10, no. 4, pp. 12–35, Oct. 1993.DOI: 10.1109/79.248551.

[3] J.-W. Choi and Y.-H. Kim, "Generation of an acoustically bright zone with an illuminated region using multiple sources" Journal of the Acoustical Society of America, vol. 111, no. 4, pp. 1695–1700, 2002. DOI:10.1121/1.1456926.

[4] W. Zhang, T. D. Abhayapala, and M. A. Poletti, "Sound field reproduction in multiple zones using loudspeaker arrays" IEEE Transactions on Audio, Speech, and Language Processing, vol. 20, no. 4, pp. 1076–1087, 2012.DOI:10.1109/TASL.2012.2183864.

[5] J. Cheer, S. J. Elliott, and M. F. Simón Gálvez, "Design and implementation of a personal audio system" Journal of the Audio Engineering Society, vol. 61, no. 3, pp. 129–138, 2013.DOI:10.17743/jaes.2013.0012.

[6] M. R. Bai and J. G. Ih, "Robust control of acoustic systems with modeling uncertainties" Journal of Sound and Vibration, vol. 230, no. 4, pp. 957–979, 2000.DOI:10.1006/jsvi.2000.3172.

[7] J. Cheer and S. J. Elliott, "Robust personal sound zones" IEEE/ACM Trans. Audio Speech Lang. Process., 2021.

[8] M. Poletti, "Sound field control in multi-zone environments: A review" Applied Acoustics, 2021.

[9] Y. Huang et al., "Adaptive sound field control under environmental uncertainty" IEEE Access, 2022.

[10] W. Zhang et al., "Robust personal sound zones under listener movement" J. Acoust. Soc. Am., 2022.

[11] S. J. Elliott, "Advances in personal audio and sound zones" IEEE Signal Processing Magazine, 2023.

[12] X. Li et al., "Data-driven sound field control methods" IEEE Access, 2023.

[13] Y. Zhu et al., "A robust hybrid ACC–PM approach for personal sound zones" Interspeech, 2025.

[14] H. Jiang and E. Choueiri, "Neural personal sound zones" arXiv, 2026.